Materials Transactions, JIM, Vol. 40, No. 3 (1999), pp. 209 to 213

Effect of Oxygen Gas Addition on Preparation of Iridium and Platinum Films by Metal-Organic Chemical Vapor Deposition

Takashi Goto, J. Roberto Vargas† and Toshio Hirai

Institute for Materials Research, Tohoku University,
2-1-1 Katahira, Aoba-ku, Sendai 980-8577, Japan

The effect of oxygen gas addition on deposition rates, composition and microstructure was investigated in preparing Ir and Pt films by metal-organic chemical vapor deposition using Ir- and Pt-acetylacetonate precursors. Without the addition of oxygen gas, 20 mass% of carbon at most was contained in the films. The carbon was amorphous, surrounding metal particles of several nanometers in diameter. The addition of oxygen gas is effective in obtaining carbon-free Ir and Pt films, and the films grow epitaxially on MgO and sapphire single crystal substrates.

(Received June 8, 1998; In Final Form November 12, 1998)

Keywords: *metal-organic chemical vapor deposition, iridium film, platinum film, oxygen gas addition, epitaxial growth*

I. Introduction

The high chemical stability and high melting point of Ir and Pt noble metals make them promising as the oxidation protection coating for structural graphite materials at temperatures above 2000 K [(1)]. Their low electrical resistivity also enables them as conducting electrode films, being useful for a range of electronic applications[(2)(3)]. Particularly, high-purity epitaxially grown films are of interest for electrodes of semiconductor devises. Metal-organic chemical vapor deposition (MOCVD) is attractive to prepare good coverage metallic films at lower deposition temperatures than those of conventional CVD. However, the low temperature deposition process often causes the incomplete thermal decomposition of precursor materials remaining impurity carbon. To overcome this problem, reactive gases (H_2 or O_2) or several complex organometallic compounds which allow no residue of carbon have been investigated in preparing Ir and Pt films by MOCVD[(1)(2)(4)-(23)]. So far, poly-crystalline Ir films with less than 1 mass% carbon impurity have been prepared from Ir-acetylacetonate[(4)] or four cyclooctadiene compounds[(6)(9)] using H_2 as a reactant gas. An epitaxial growth of Pt films from Pt-acetylacetonate has been achieved on single crystals of $KTaO_3$ and $SrTiO_3$[(13)]. In this paper, we report the preparation of high purity Ir and Pt films by MOCVD using Ir- and Pt-acetylcetonate precursors and oxygen as a reactant gas, and describe the epitaxial relationship between the films and the single crystal substrates.

II. Experimental

A schematic diagram of the horizontal hot-wall MOCVD apparatus is shown in **Fig. 1**. Argon gas was used as the carrier gas at a flow rate (FR_{Ar}) of 8.3×10^{-7} $m^3 s^{-1}$. Oxygen gas was added into the source vapor through a separated inlet near the substrate place at flow rates (FR_{O_2}) from 0 to 2×10^{-7} $m^3 s^{-1}$. Metal-acetylacetonate precursors [$(CH_3\text{-}COCHCO\text{-}CH_3)_3Ir$ and $(CH_3\text{-}COCHCO\text{-}CH_3)_2Pt$] were used as source materials. Deposition temperature (T_{dep}) was varied from 673 to 1073 K, and total pressure (P_{tot}) was controlled from 0.27 to 13 kPa. The precursor temperature (T_{prec}) was kept constant at 453 K, and depositions were performed for 1.2 to 10.8 ks. Quartz glass, (100) MgO and (0001), $(11\bar{2}0)$ and $(01\bar{1}2)$ sapphire single crystals were used as substrates. **Table 1** summarizes the deposition conditions for preparing Ir and Pt films. Deposition rates were determined from thickness measurements using a Talystep thickness tester. Crystal structure and composition of the films were analyzed by X-ray diffraction

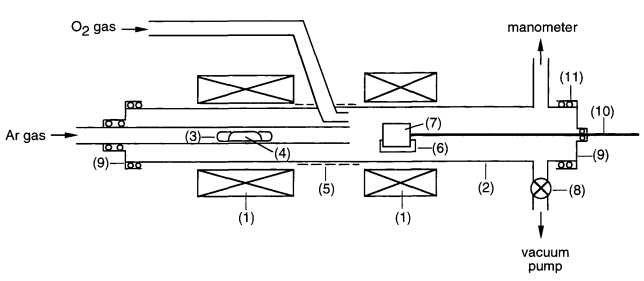

Fig. 1 Schematic diagram of the horizontal hot-wall CVD apparatus. (1) furnace, (2) quartz tube, (3) quartz reservoir, (4) precursor powder, (5) ribbon heater, (6) substrate holder, (7) substrate, (8) needle valve, (9) flange, (10) thermocouple, (11) o-ring seal.

† Graduate Student, Tohoku University, Present address: ESIQIE-IPN, AP. 75-874, Mexico.

Table 1 Deposition conditions.

Deposition temperature, T_{dep}/K	673 to 1073
Total gas pressure, P_{tot}/kPa	0.27 to 13
Precursor temperature, T_{prec}/K	453
Gas flow rates,	
Argon gas, FR_{Ar}/m^3 s^{-1}	8.3×10^{-7}
Oxygen gas, FR_{O_2}/m^3 s^{-1}	0 to 1.7×10^{-7}
Time, t/ks	1.2 to 10.8

(XRD) using Cu Kα radiation and Auger electron spectroscopy (AES). Scanning electron microscopy (SEM) was used to observe the surface and cross-section of films. The microstructure of deposits removed from the substrates was studied by transmission electron microscopy (TEM).

III. Results and Discussion

Figure 2 shows the effect of CVD conditions on the appearance of Ir films prepared without the addition of oxygen gas on quartz glass substrates. Below $T_{dep}=673$ K, no films were obtained independent of P_{tot}. In the range between $T_{dep}=647$ and 1073 K, mirror like films were obtained at $P_{tot}=0.27$ kPa. This T_{dep} range became narrower with increasing P_{tot}. Higher P_{tot} conditions yield black powdery deposits. Mirror-like Ir films prepared at $T_{dep}=873$ K and $P_{tot}=0.27$ to 0.67 kPa exhibited XRD peaks for Ir (111), Ir (200) and Ir (220) at $2\theta=40.7°$, 47.3° and 69.2°, respectively, indicating no specific preferred orientation (see **Figs. 3**(a)(b)). Black powdery deposits showed a weak XRD peak for Ir (111) (Fig. 3(c)), or no observable peak for Ir (Fig. 3(d)).

Figure 4 shows XRD patterns of Pt films prepared on quartz glass substrates at $P_{tot}=0.27$ kPa, $T_{dep}=773$ K and $FR_{O_2}=0$, 5×10^{-8} and 2×10^{-7} m^3 s^{-1}. Pt films prepared without the addition of oxygen gas exhibit broader XRD peaks than those prepared at $FR_{O_2}>5\times10^{-8}$ m^3 s^{-1}. Broadening of XRD peaks could be originated by a small average grain size. A higher addition of oxygen gas, $FR_{O_2}=2\times10^{-7}$ m^3 s^{-1}, yields Pt films highly oriented in [111] direction. There is a general trend that the preferred orientation occurs in the closest packed plane (*i.e.*, (111) plane in the fcc crystals) in order to minimize the surface energy[24]. Pangarov indicated that the preferred orientation of fcc crystals changes from (001) to (110) to (111) with decreasing deposition rates (or supersaturation)[25]. The oxygen addition reduced the deposition rates significantly as shown in Fig. 6. The (111) orientation in the present study may be understood by the general trend and the Pangarov's model. Poly-crystal-

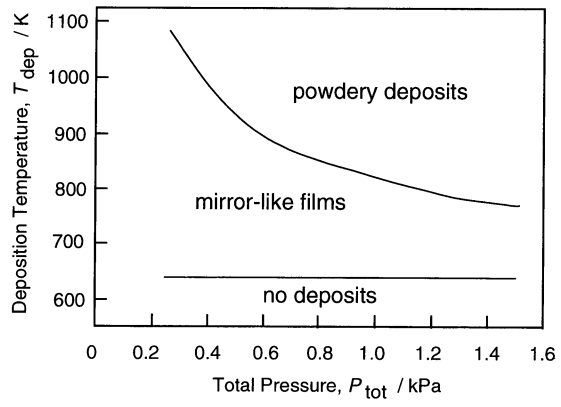

Fig. 2 Effect of CVD conditions on the appearance of Ir films prepared without the addition of oxygen gas on quartz glass substrates.

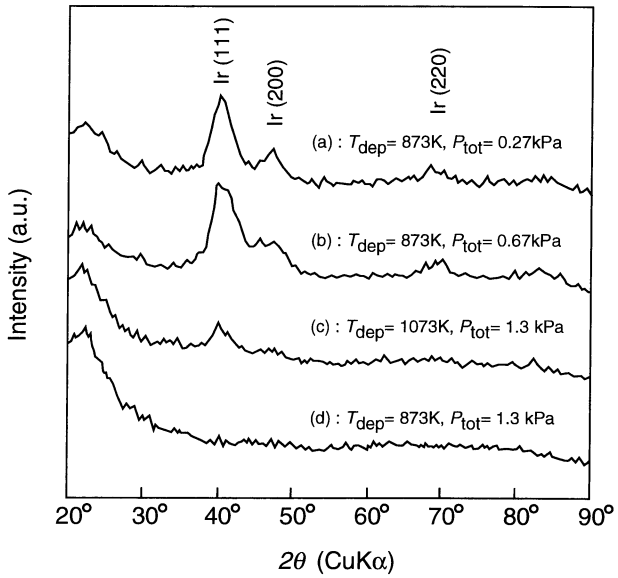

Fig. 3 XRD patterns of Ir films prepared on quartz glass substrates without the addition of oxygen gas.
(a), (b) mirror-like films and (c), (d) powdery deposits.

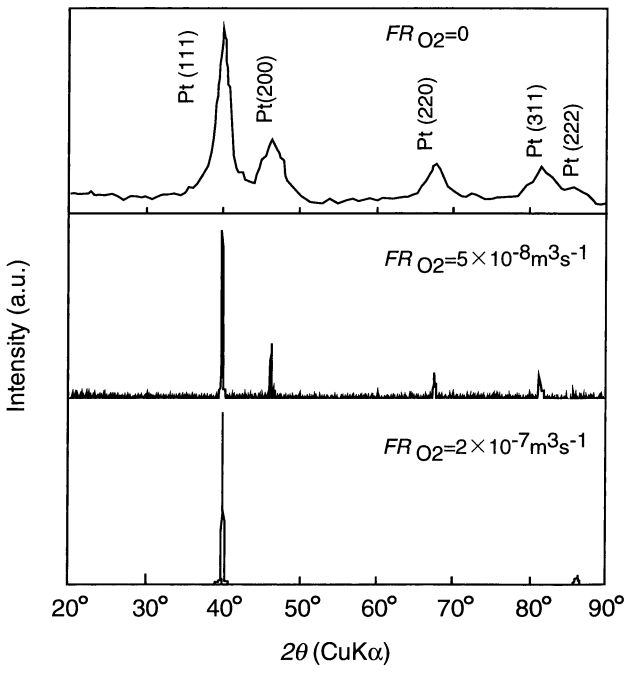

Fig. 4 XRD patterns of Pt films prepared on quartz glass substrates at $P_{tot}=0.27$ kPa, $T_{dep}=773$ K and $FR_{O_2}=0$, 5×10^{-8} and 2×10^{-7} m^3 s^{-1}.

line Pt films with the (111) orientation on fused quartz and (100) Si substrates have been previously reported in literature[13]. In the case of Ir films, a small addition of oxygen gas, $FR_{O_2}=5\times10^{-8}$ m^3 s^{-1}, allowed for sharper XRD peaks than those observed in Fig. 3. At higher oxygen gas additions, $FR_{O_2}>5\times10^{-8}$ m^3 s^{-1}, IrO_2 was formed. The films obtained with the addition of oxygen gas were silver colored with mirror-like surfaces.

Figure 5 shows Auger spectra before and after argon sputtering for Ir films prepared on quartz glass substrates at $T_{dep}=873$ K and $P_{tot}=0.27$ kPa. AES results indicate that the surfaces of Ir and Pt films prepared without the addition of oxygen gas were contaminated with carbon and oxygen. Although the film surfaces were sputtered with argon (2 kV, 600 s), carbon was detected in these films. The estimated carbon content from the intensity ratio of Ir to C signals were 20 mass% at most. In contrast, for films prepared at $FR_{O_2}=5\times10^{-8}$ m^3 s^{-1} for Ir, and $FR_{O_2}=2\times10^{-7}$ m^3 s^{-1} for Pt, no observable signals from carbon or oxygen were detected after their surfaces were sputtered with argon. AES and XRD results indicate that the addition of oxygen gas was effective in obtaining highly pure and well-crystallized films from Ir- and Pt-acetylacetonate precursors. MOCVD Ir and Pt films of high purity (less than 1 mass% carbon) have been previously reported mostly using H_2 as a reactant gas, or otherwise by using complex organometallic precursors. The resulting structure and film composition are summarized in **Table 2.**

Figure 6 shows the effect of oxygen gas addition on Ir

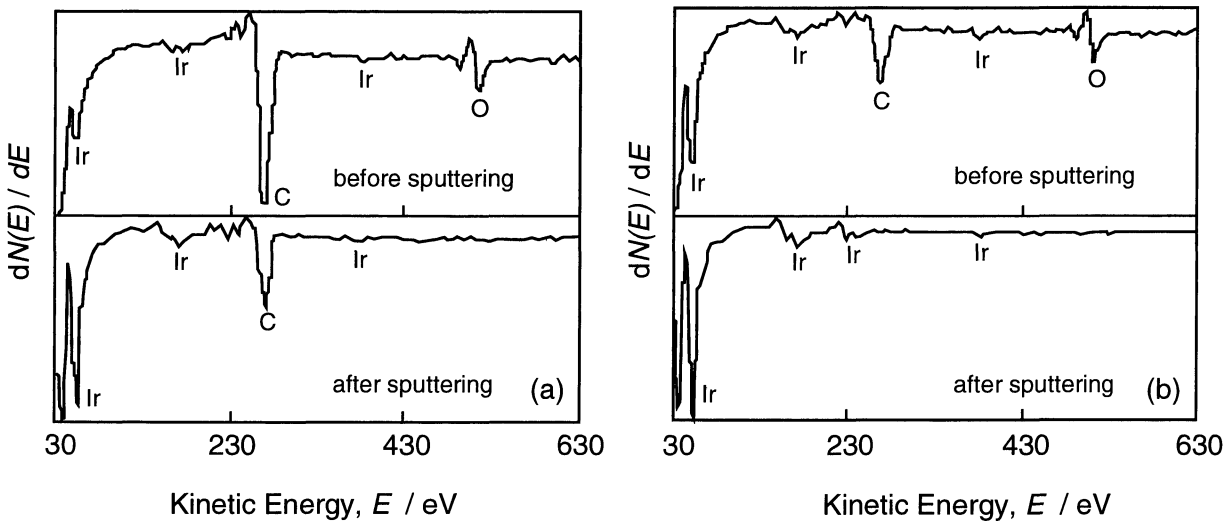

Fig. 5 Auger spectra before and after argon sputtering (2 kV, 600 s) for Ir films prepared on quartz glass substrates at $T_{dep}=873$ K, $P_{tot}=0.27$ kPa.
(a) without the addition of oxygen gas, (b) with the addition of oxygen gas at $FR_{O_2}=5\times10^{-8}$ m^3 s^{-1}.

Table 2 Ir and Pt organometallic precursors reported in literatures.

Precursor	Substrate	Reactant gas	Film composition	Structure	Ref.
$Ir(acac)_3$	Glass, quartz	H_2	C, O free	Crystalline	1-2, 4-5
Ir(acac)(cod)	Cu	H_2	99 mass%Ir		6
$Ir(allyl)_3$	Glass	H plasma	97 mass%Ir	Crystalline	7-8
(MeCp)Ir(cod)	Fused silica	H_2	<1 mass%C	Crystalline	9
(Cp)Ir(cod)	Fused silica		<1 mass%C	Crystalline	9-10
$[Ir(\mu\text{-OMe})(cod)]_2$	Cu	H_2	95 mass%Ir		6
$[(cod)Ir(\mu\text{-OAc})]_2$	Fused silica	vacuum	<1 mass%C, O	Crystalline	9
$CpIr(C_2H_4)_2$	(100) Si	H_2	<1 mass%C	Crystalline	11
Ir(dpm)(cod)	Quartz	H_2	98 mass%Ir		12
$Pt(acac)_2$	$KTaO_3$, $SrTiO_3$	O_2		(100) epitaxial	13-14
$Pt(CO)_2Cl_2$	Si	H_2	99.6 mass%Pt	Crystalline	14
$Pt(PF_3)_4$	Sapphire	H_2	P-impurity	Preferred orientation	14-16
$Pt(allyl)_2$					17
$CpPtMe_3$	(100) Si	H_2	<1 mass%C, O	Preferred orientation	8, 18-20
$(MeCp)PtMe_3$	(100) Si	H_2	<1 mass%C	Preferred orientation	8, 21
Cis~$[PtMe_2(MeNC)_2]$					22
$Pt(HFacac)_2$	Glass		96 mass%Pt	Amorphous	23

acac=acetylacetonate; Cp=cyclopentadienyl; MeCp=methylcyclopentadienyl; cod=1,5-cyclooctadiene; OAc=acetate; OMe=methoxide; HF=hexafluoro.

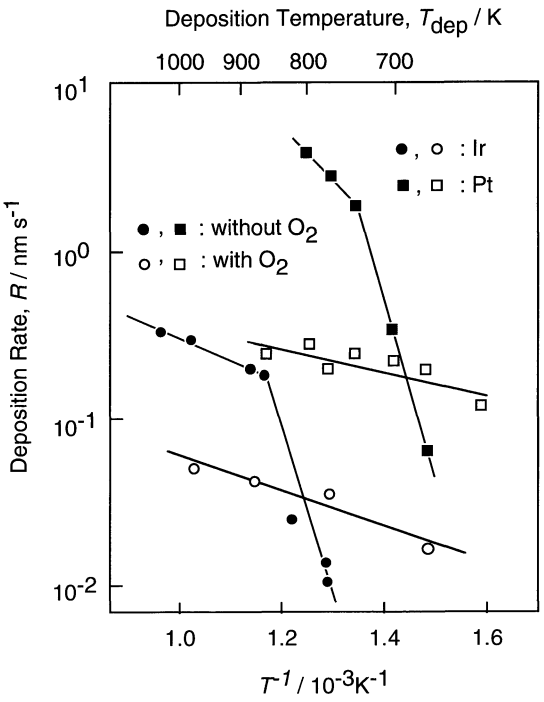

Fig. 6 Dependence of deposition rates on the deposition temperature without the addition of oxygen gas and with the addition of oxygen gas at $FR_{O_2}=5\times10^{-8}$ m^3 s^{-1} for Ir and $FR_{O_2}=2\times10^{-7}$ m^3 s^{-1} for Pt films.

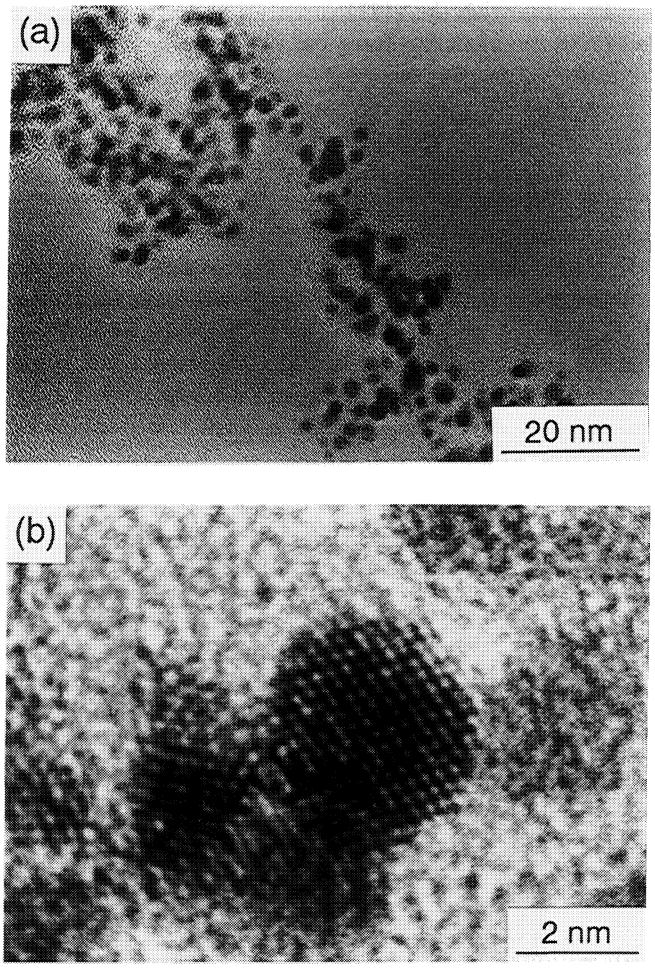

Fig. 7 TEM images for the Ir film prepared without the addition of oxygen gas at $T_{dep}=873$ K and $P_{tot}=0.4$ kPa.
(b) is a higher magnification of (a).

and Pt deposition rates. Without the oxygen gas addition, two growth regimes were distinguished in the relationship between logarithmic deposition rate and reciprocal temperature. The activation energy for Ir at $T_{dep}<873$ K was 160 kJ mol^{-1}, and that for Pt at $T_{dep}<743$ K was 200 kJ mol^{-1}. At higher temperatures, the activation energies were 24 and 60 kJ mol^{-1} for Ir and Pt, respectively. It is well-known that the rate-controlling step could change from a reaction-controlled regime to a diffusion-controlled regime with increasing temperature[26]. The activation energy associated with the reaction controlled regime is usually more than several tens kJ mol^{-1}. The present values of 160 to 200 kJ mol^{-1} at low temperatures suggest the reaction-controlled regime. The values of 24 to 60 kJ mol^{-1} might be rather high than that for the diffusion-controlled regime[12]. It is not clear that these values are correlated to the chemical reaction or the diffusion process.

With the addition of oxygen gas ($FR_{O_2}=5\times10^{-8}$ m^3 s^{-1} for Ir and $FR_{O_2}=2\times10^{-7}$ m^3 s^{-1} for Pt), the activation energies were 13 and 20 kJ mol^{-1} for Ir and Pt films, respectively. Under these conditions, we confirmed that the deposition rates depended on the total gas pressure and gas flow rate. Therefore, these values could correspond to the values for the diffusion-controlled regime. The addition of oxygen gas decreased Ir and Pt deposition rates significantly. Formation of volatile metal oxide species and denser films could cause the lower deposition rates. In the whole temperature range, deposition rates of Pt were higher than those of Ir. Higher vapor pressure and higher metal content of the Pt precursor could explain the higher deposition rates of Pt films. Vapor pressures at 453 K and metal contents for Ir- and Pt-acetylacetonates are about 13 and 133 Pa[1], and 39.3 mass%Ir and 49.6 mass%Pt, respectively.

Figure 7 illustrates TEM images taken from the Ir film prepared without the addition of oxygen gas at $T_{dep}=873$ K and $P_{tot}=0.4$ kPa. Crystalline particles with several nanometers in diameter were observed to be parallel to the densest plane of (111) Ir. Broad Ir XRD peaks (see Fig. 3) appear to be due to the small size of crystalline particles revealed in this image. The amorphous phase around Ir particles is associated with carbon detected by AES analysis. The TEM image of the amorphous phase could well correspond to that of amorphous carbon[27].

High purity condition of Ir and Pt films achieved by the addition of oxygen allowed for their epitaxial growth on (100) MgO and (0001), (11$\bar{2}$0) and (01$\bar{1}$2) sapphire single crystal substrates. The film orientation and epitaxial relationships were determined by XRD and X-ray pole figures. **Table 3** summarizes the epitaxial relationships between Ir, Pt films and single crystal substrates.

Table 3 Epitaxial relationships between Ir, Pt films and single crystal substrates.

Substrate	Epitaxial relationship
MgO (100)	Ir, Pt (100)//MgO (100) and Ir, Pt [110]//MgO [110]
Sapphire ($11\bar{2}0$)	Ir (100)//sapphire ($11\bar{2}0$) and Ir [110]//sapphire [$1\bar{1}00$]
	Pt (111)//sapphire ($11\bar{2}0$) and Pt [$\bar{2}11$]//sapphire [0001]
	Pt [$2\bar{1}\bar{1}$]//sapphire [0001]
Sapphire (0001)	Pt (111)//sapphire (0001) and Pt [$2\bar{1}\bar{1}$]//sapphire [$10\bar{1}0$]
	Ir, Pt (111)//sapphire (0001) and Ir, Pt [$\bar{2}11$]//sapphire [$\bar{1}\bar{1}20$]
	Ir, Pt [$2\bar{1}\bar{1}$]//sapphire [$\bar{1}\bar{1}20$]
Sapphire ($01\bar{1}2$)	Ir, Pt (111)//sapphire ($01\bar{1}2$) and Ir, Pt [$\bar{1}10$]//sapphire [$1\bar{2}10$]

IV. Conclusions

The addition of oxygen gas was effective in obtaining high-purity and good crystalline quality Ir and Pt films by MOCVD from Ir- and Pt-acetylacetonate precursors at temperatures between 773 and 873 K. Without the addition of oxygen gas, carbon containing films, 20 mass% at most, surrounding crystalline metallic particles were obtained. Pt deposition rates were higher than those of Ir because of a higher vapor pressure and a higher metal content of Pt-acetylactonate. High-purity Ir and Pt films are epitaxially grown on MgO and sapphire single-crystal substrates.

REFERENCES

(1) J. T. Harding, V. Fray, R. H. Tufflas and R. B. Kaplan: AFRPL TR-86-099, (1987).
(2) V. G. Bessergenev, N. V. Gelfond, I. K. Igumenov, S. Sh. Llyasov, R. D. Kangiev, Yu. A. Kovalevskaya, V. S. Kravchenko, S. A. Slobodyan, V. I. Motorin and A. F. Shestak: Supercond. Sci. Technol., **4** (1991), 273.
(3) M. Adachi, T. Matsuzaki, T. Yamada, T. Shiosaki and A. Kawabata: Japan. J. Appl. Phys., **26** (1987), 550.
(4) N. V. Gelfond, I. K. Igumenov, A. I. Boronin, V. I. Bukhtiyarov, M. Yu. Smirnov, I. P. Prosvirin and R. I. Kwon: Surface Sci., **275** (1992), 323.
(5) N. V. Gelfond, F. V. Tuzikov, I. K. Igumenov: Thin Solid Films, **227** (1993), 144.
(6) J. A. Papke and R. D. Stevenson: Proc. Conf. Chem. Vapor Dep. Refract. Metals, Alloys, Compounds, (1967), 193.
(7) D. C. Smith, S. G. Pattillo, N. E. Elliot, T. G. Zocco, C. J. Burns, J. R. Laia and A. P. Sattelberger: Mat. Res. Soc. Symp. Proc., Vol. 168, (1990), 369.
(8) H. D. Kaesz, R. S. Williams, R. F. Hicks, Y. A. Chen, Z. Xue, D. Xu, D. K. Shuh and H. Thridandam: Mat. Res. Soc. Symp. Proc., Vol. 131, (1989), 395.
(9) J. B. Hoke, E. W. Stern and H. H. Murray: J. Mater. Chem., **1** (1991), 551.
(10) B. A. Macklin and P. A. LaMar: AFML-TR-67-195, (1968).
(11) J. S. Cohan, H. Yuan, R. S. Williams and J. I. Zink: Appl. Phys. Lett., **60** (1992), 1402.
(12) T. Gerfin, W. J. Halg, F. Atamy, K. H. Dahmen: Thin Solid Films, **241** (1994), 352.
(13) B. S. Kwak, P. N. First, A. Erbil, B. J. Wilkens, J. D. Budai, M. F. Chisholm and L. A. Boatner: J. Appl. Phys., **72** (1992), 3735.
(14) M. J. Rand: J. Electrochem. Soc., **120** (1973), 686.
(15) M. J. Rand: J. Electrochem. Soc., **122** (1975), 811.
(16) D. S. Y. Hsu: Appl. Phys. Lett., **59** (1991), 2192.
(17) J. E. Gosum, D. M. Pollina, J. A. Jensen and G. S. Girolami: J. Am. Chem. Soc., **110** (1988), 2688.
(18) Y. Chen, H. D. Kaesz, H. Thridandam and R. F. Hicks: Appl. Phys. Lett., **53** (1988), 1591.
(19) L. V. Koplitz, D. K. Shuh, Y.-J. Chen, R. S. Williams and J. I. Zink: Appl. Phys. Lett., **53** (1988), 1705.
(20) E. Feurer, S. Kraus and H. Suhr: J. Vac. Sci. Technol. A, **7** (1989), 2799.
(21) Z. Xue, M. J. Strouse, D. K. Shuh, C. B. Knobler, H. D. Kaesz, R. F. Hicks and R. S. Williams: J. Am. Chem. Soc., **111** (1989), 8779.
(22) B. Nixon, P. R. Norton, E. C. Ou, R. J. Puddephatt, S. Roy and P. A. Young: Chem. Mater., **3** (1991), 222.
(23) C. Garrido and H. van den Bergh: Appl. Phys. A, **53** (1991), 265.
(24) Y. Imai, M. Mukaida, A. Watanabe and T. Tsunoda: Thin Solid Films, **300** (1997), 305.
(25) N. A. Pangarov: Electrochim. Acta., **7** (1962), 139.
(26) J. M. Blocher, Jr.: *Vapor Deposition*, Ed. by C. F. Powell, J. H. Oxley and J. M. Blocher, Jr., John Wiley, New York, (1966), p. 3.
(27) J. B. Donnet and A. Voet: *Carbon Black, Physics, Chemistry and Elastomer Reinforcement*, M. Dekker, New York, (1976).